4-Tritylbenzoic acid. A molecular scaffold for wheel-and-axle host–guest inclusion compounds with a supramolecular axis

Ram K. R. Jetti,[a] Feng Xue,[b] Thomas C. W. Mak *[b] and Ashwini Nangia *[a]

[a] *School of Chemistry, University of Hyderabad, Hyderabad 500 046, India. E-mail: ansc@uohyd.ernet.in*
[b] *Department of Chemistry, The Chinese University of Hong Kong, Shatin, New Territories, Hong Kong SAR, P. R. China. E-mail: tcwmak@cuhk.edu.hk*

Received (in Cambridge, UK) 14th December 1999, Accepted 22nd March 2000
Published on the Web 9th May 2000

4-Tritylbenzoic acid crystallises *via* the carboxy dimer supramolecular synthon to produce a wheel-and-axle host lattice that includes different aromatic solvents in its microporous framework. The clathrate structures were characterised by single crystal X-ray diffraction. Solvents like xylenes, chlorobenzene and anisole are included in a channel of cross-sectional area 42 Å^2 with 2 : 1 host–guest stoichiometry while mesitylene occupies a channel of 71 Å^2 as a 1 : 1 clathrate. The host architecture is robust and yet adaptive. The carboxy dimer synthon together with the phenyl–phenyl interactions (edge-to-face, **ef** and offset face-to-face, **off**) produce recurring, zigzag tapes of wheel-and-axle supermolecules. A plethora of aromatic **ef** and **off** motifs in the intra- and inter-tape regions modulate the cavity area to accommodate solvents of different size/shape. The ability to tune the pore volume and still retain the target wheel-and-axle topology is a notable feature in this family of isomorphous structures. The unsolvated acid adopts a different crystal packing with the triphenylmethyl groups filling the voids in the structure.

Introduction

The design of crystalline clathrates and microporous solids is a contemporary goal in crystal engineering.[1] The control of target architectures in the solid state is challenging because there are no general methods for the prediction of organic crystal structures by computational methods. Furthermore, the effect of change in substituent in the host structure or in the guest species on crystal packing is even more difficult to predict. The extent to which a supramolecular structure is sensitive to perturbation by the guest could vary: some structures retain their packing features and architecture for a series of guest molecules with only small changes in lattice parameters,[2] while other hosts are adaptive and reorganise to produce isomeric structures with a change in guest size/shape.[3] Interpenetration[4] of the host lattice produces global structural changes and is unwanted in the design of porous frameworks.

Strategies for the self-assembly of organic host frameworks rely on the programmed recognition between topologically and chemically complementary functional groups through non-covalent interactions, referred to as supramolecular synthons.[5] Among the numerous non-covalent interactions in the repertoire of the supramolecular chemist, hydrogen bonding, strong[6] as well as weak,[7] serves as a reliable adhesive to produce specific and robust recognition patterns. Some recent examples of crystalline organic clathrates assembled *via* O–H···O and C–H···O hydrogen bonds are helical tubulands,[3a,8] roof-shaped hydroxy hosts,[9] binaphthyl dicarboxylic acids,[10] tartaric and lactic acid derived diols,[11] anthracenebisresorcinol[1d,2b,3b] and calix[4]resorcinarenes.[12] Other approaches adopted for generating open networks make use of metal–ligand co-ordination[1e,13] and cation–anion recognition.[14]

The wheel-and-axle class of host compounds[15] have a long, linear axis with large, rigid substituents at both ends. The traditional approach has been to synthesize molecules with bulky terminal groups (wheels) which are connected by linearly fused rings or triple bonds (axle).[16] For example, in host **1** the trityl end-groups prevent close packing around the acetylene spacer, thereby creating voids that are occupied by a guest component, usually extracted from the crystallisation solvent. Host **1** forms a 1 : 1 clathrate with chloroform and its higher congeners with phenyl/biphenyl groups include aromatic guests.[16b]

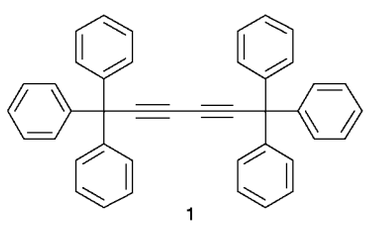
1

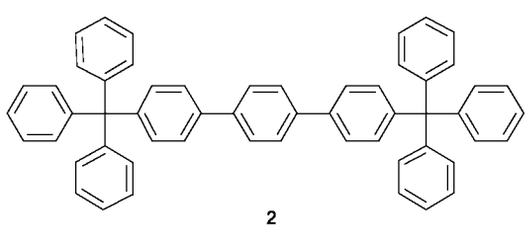
2

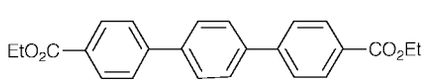

3

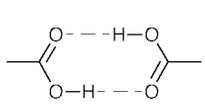

4

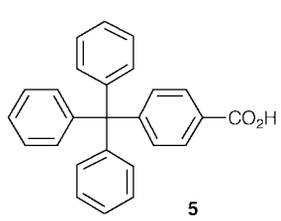

5

Based on the above considerations, it was reasoned that the aromatic hydrocarbon **2** should function as a wheel-and-axle host. However, the synthesis of compound **2** was expected to

be both long and difficult though a possible route could be envisioned starting from the known diester **3**.†[17,18] At this point, 4-(triphenylmethyl)benzoic acid **5** suggested itself as a surrogate supermolecule of host **2** based on the topological equivalence between a *para*-substituted phenyl ring and the carboxylic acid dimer supramolecular synthon **4**.[5,19] While this work was in progress, the self-assembly of [3]pseudorotaxanes *via* the carboxy dimer synthon and the similarity of the dimer structure with the corresponding *p*-phenyl[3]pseudorotaxane was reported.[19] These encouraging factors coupled with the low solubility expected of a polycyclic aromatic hydrocarbon such as **2** directed studies towards acid **5** as a new wheel-and-axle scaffold with a non-covalent axis.[20] A conceptual advance in our design of inclusion compound **5** is that the host itself is a supermolecule which in turn must include guests in its voids to produce the wheel-and-axle structure. In effect, self-assembly not only of the multi-component host lattice but also of guest inclusion in the voids has to be premeditated.

In the present study, crystal structures of wheel-and-axle host–guest compounds of 4-tritylbenzoic acid **5** with a variety of aromatic solvents such as xylenes, chlorobenzene, bromobenzene, nitrobenzene, anisole and mesitylene are reported and their hydrogen bonding patterns analysed. Two types of crystal structures with different pore sizes are obtained: xylenes, chlorobenzene or anisole are included in channels of cross-section *ca.* 42 Å^2 with a 2:1 host–guest stoichiometry while the 1:1 mesitylene clathrate has a larger channel of 71 Å^2 area. Further, the guest-free form of **5** shows a different crystal packing. Thermochemical data (DSC, TG) of **5**·xylene, a prototype clathrate in this family, are discussed.

Results and discussion

4-Tritylbenzoic acid was synthesized in 35% yield by homologation of the known iodo derivative **6** with CuCN to **7** followed by hydrolysis with KOH to provide the desired acid **5**.[18] The acid was recrystallised from CH_2Cl_2 and characterised by its satisfactory IR and NMR spectra.

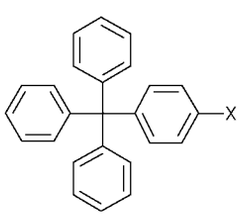

6: X = I
7: X = CN
5: X = CO_2H

Inclusion compounds of 5

Recrystallisation of acid **5** from mixed xylenes‡ at room temperature afforded inclusion compounds of 2:1 stoichiometry that crystallise in the triclinic space group $P\bar{1}$ with $Z = 2$ (Table 1).[20] The crystal structure of **5**·xylene shows the centrosymmetric carboxylic acid dimer synthon **4** (O–H · · · O: *d* 1.67 Å, θ 168.7°, Fig. 1, Table 2). These dimers are packed as zigzag tapes through aromatic edge-to-face (**ef**) and offset face-to-face (**off**) interactions between pairs of phenyl rings.[21] The concerted stabilisation from the dimer synthon and the phenyl–phenyl interactions produces the target wheel-and-axle architecture with the voids being occupied by xylene molecules (Fig. 1). The model for least squares refinement assumes partial occupancies of each of the three isomeric xylenes in the crystal. This was

† Addition of an excess of PhMgBr to 4,4″-bis(ethoxycarbonyl)-1,1′:4′,1″-terphenyl **3** (ref. 17) will provide the requisite tertiary diol for elaboration to **2** using the protocol delineated in ref. 18.

‡ Xylene is a mixture of the three isomers and traces of ethylbenzene. This was used as such for recrystallisation. Interestingly, pure ethylbenzene is also included in crystals of **5** but it is lost within a few days (NMR); no single crystal data could be obtained on this sample.

Table 1 Crystallographic data and structure refinement parameters

	5·Xylene	**5**·PhCl	**5**·*o*-Xylene	**5**·*m*-Xylene	**5**·*p*-Xylene	**5**·Mesitylene	**5**·Anisole	**5**·PhBr	**5**·$PhNO_2$	Unsolvated **5**
Chemical formula	$C_{26}H_{20}O_2$·0.5C_8H_{10}	$C_{26}H_{20}O_2$·0.5C_6H_5Cl	$C_{26}H_{20}O_2$·0.5C_8H_{10}	$C_{26}H_{20}O_2$·0.5C_8H_{10}	$C_{26}H_{20}O_2$·0.5C_8H_{10}	$C_{26}H_{20}O_2$·C_9H_{12}	$C_{26}H_{20}O_2$·0.5C_7H_8O	$C_{26}H_{20}O_2$·0.5C_6H_5Br	$C_{26}H_{20}O_2$·0.5$C_6H_5NO_2$	$C_{26}H_{20}O_2$
Formula wt.	417.50	420.69	417.50	417.50	417.50	484.61	418.77	442.92	425.98	364.42
Crystal system	Triclinic	Triclinic	Triclinic	Triclinic	Triclinic	Triclinic	Triclinic	Triclinic	Triclinic	Orthorhombic
Space group	$P\bar{1}$ (no. 2)	$P\bar{1}$ (no. 2)	$P\bar{1}$ (no. 2)	$P\bar{1}$ (no. 2)	$P\bar{1}$ (no. 2)	$P\bar{1}$ (no. 2)	$P\bar{1}$ (no. 2)	$P\bar{1}$ (no. 2)	$P\bar{1}$ (no. 2)	*Pbca* (no. 61)
a/Å	7.3270(10)	7.3100(10)	7.368(1)	7.329(1)	7.241(2)	7.390(1)	7.310(1)	7.3066(2)	7.340(2)	7.390(2)
b/Å	9.042(2)	8.9940(10)	9.010(1)	9.044(1)	9.011(2)	13.637(1)	8.998(1)	8.9943(2)	8.982(2)	15.477(2)
c/Å	18.534(4)	18.454(2)	18.522(1)	18.547(1)	18.916(3)	14.349(1)	18.464(1)	18.4973(5)	18.366(4)	33.858(2)
α/°	88.09(3)	89.190(10)	88.00(1)	88.54(1)	84.25(2)	75.92(1)	89.98(1)	89.764(1)	89.33(3)	
β/°	85.07(3)	85.750(10)	84.97(1)	85.33(1)	87.25(2)	81.64(1)	86.26(1)	85.946(1)	86.14(3)	
γ/°	68.07(3)	68.230(10)	67.94(1)	67.33(1)	66.66(2)	85.16(1)	67.50(1)	67.868(1)	67.55(3)	
Z	2	2	2	2	2	2	2	2	2	8
V/Å^3	1134.8(4)	1123.5(2)	1135.2(2)	1133.1(2)	1127.5(2)	1385.9(2)	1119.2(2)	1122.82(5)	1116.4(4)	3872.5(14)
T/K	294	294	294	294	294	294	294	294	294	294
μ/mm^{-1}	0.084	0.134	0.084	0.084	0.075	0.070	0.088	0.964	0.081	0.078
mp/°C	268–269	244–245	245–246	245–246	246–248	256–258	269–270	269–270	268–270	269–271
R_1 ($I > 2\sigma(I)$)	0.0660	0.0755	0.0576	0.0519	0.0532	0.0493	0.0525	0.0886	0.0905	0.0494
wR_2 (all)	0.2253	0.2716	0.1733	0.1925	0.1716	0.1585	0.1664	0.2802	0.2924	0.0890
N Measured	3986	4398	3983	3982	4414	4537	4375	3797	3895	2936
N Unique (R_{int})	3986 (0.0220)	4396 (0.0357)	3980 (0.0559)	3976 (0.0264)	4414 (0.0273)	4537 (0.0272)	4373 (0.0333)	3797 (0.0248)	3895 (0.0220)	1503 (0.0605)
C_k	0.70	0.68	0.67	0.68	0.67	0.65	0.68	0.68	0.69	0.68

Table 2 Geometry of hydrogen bonds in host–guest structures **5**

Guest	Interaction[a]	H···O/Å	O/C···O/Å	O/C–H···O/°
Xylenes	O(1)–H···O(2)	1.67	2.637(5)	168.7
	C(21)–H···O(1)	2.85	3.844(5)	152.2
PhCl	O(1)–H···O(2)	1.65	2.619(5)	166.8
	C(21)–H···O(1)	2.84	3.841(5)	153.9
o-Xylene	O(2)–H···O(1)	1.64	2.619(4)	173.1
	C(14)–H···O(2)	2.83	3.827(5)	153.2
	C(31)–H···O(1)	2.76	3.745(8)	150.6
m-Xylene	O(2)–H···O(1)	1.67	2.646(3)	170.7
	C(14)–H···O(2)	2.84	3.832(3)	152.8
p-Xylene	O(1)–H···O(2)	1.68	2.650(3)	167.8
	C(10)–H···O(1)	2.77	3.827(3)	164.1
	C(29)–H···O(2)	2.88	3.955(4)	169.6
Mesitylene	O(1)–H···O(2)	1.65	2.630(3)	169.3
	C(22)–H···O(2)	2.94	4.011(4)	167.8
	C(30)–H···O(2)	2.77	3.824(5)	163.9
	C(34)–H···O(1)	2.84	3.910(5)	170.2
Anisole	O(2)–H···O(1)	1.66	2.628(3)	167.5
	C(14)–H···O(2)	2.77	3.790(3)	156.5
PhBr	O(1)···O(2)	—[b]	2.631(4)	—[b]
	C(13)–H···O(1)	2.79	3.802(4)	155.2
$PhNO_2$	O(1)–H···O(2)	1.67	2.631(4)	165.2
	C(19)–H···O(2)	2.81	3.822(5)	155.7
None	O(1)–H···O(2)	1.68	2.656(5)	169.6
	C(7)–H···O(2)	2.76	3.631(5)	137.2
	C(18)–H···O(1)	2.88	3.749(5)	137.5

[a] O–H and C–H distances are neutron-normalised (0.983, 1.083 Å). [b] H-atom could not be located.

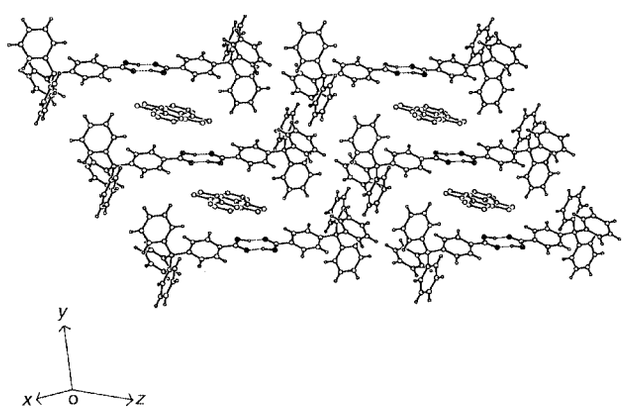

Fig. 1 Crystal structure of compound **5**·xylene (mixed) down [100] to show the wheel (trityl groups) and supramolecular axle **4**. The channels are filled with disordered xylene molecules. Notice the profusion of phenyl–phenyl interactions.

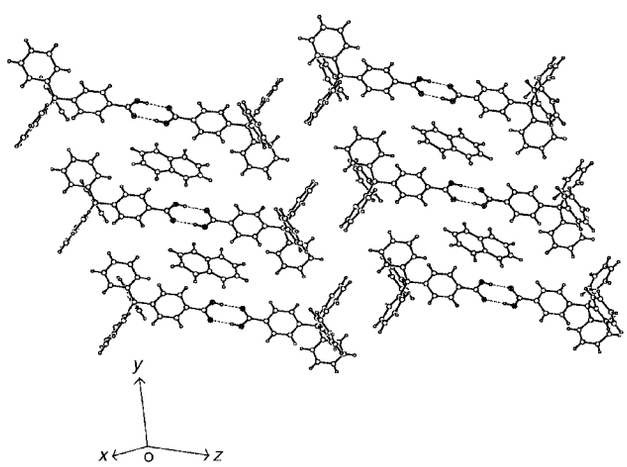

Fig. 2 Crystal structure of compound **5**·anisole down [100]. Notice the similarity with Fig. 1. The disordered guest mimics a naphthalene molecule.

confirmed with ^{1}H NMR ($CDCl_3$) that shows equal amounts of the three isomers present in the crystal. Diffraction quality crystals, obtained from chlorobenzene (**5**·PhCl, 2:1), are isomorphous with the xylene solvate and contain disordered guest molecules.[20] The facile inclusion of guests in the wheel-and-'supramolecular'-axle microporous framework encouraged us to examine recrystallisation of host **5** from other aromatic solvents. The crystallographic data and intermolecular interactions in the structures are summarised in Tables 1 and 2.

Wheel-and-axle host–guest 2:1 adducts were obtained from isomerically pure *o*- and *m*-xylene, anisole, bromobenzene and nitrobenzene. The crystal structure of **5**·anisole, displayed in Fig. 2, exhibits the dimer synthon **4** (1.66 Å, 167.5°) with the disordered guest molecules included in its porous lattice. In these isomorphous structures the guest molecules are orientationally disordered. The treatment of guest disorder and site-occupancy factor (s.o.f.) of solvent atoms in each structure was done differently to obtain good match between observed and calculated electron densities (*R* factor). Details are provided in the Experimental section. Structure solution and refinement were uneventful and yielded converged models with good *R* factors (0.04–0.06) for mixed xylenes, *o*-, *m*-, and *p*-xylene, anisole, and mesitylene. Though the *R* values in some cases are slightly higher (>0.07 for PhCl, PhBr and $PhNO_2$ solvates, Table 1), these structures are included in the discussion because they are part of the same isomorphous host–guest family. A possible reason for the high *R* could be guest disorder, and so this phenomenon was examined next.

There could be two possible reasons for guest disorder in the host channel: (1) the host cavity size is sufficiently large for the guest to occupy alternative orientations; (2) the small unsymmetrical guest adapts to the inversion symmetry imposed by the larger host lattice. In order to distinguish between these situations, acid **5** was recrystallised from *p*-xylene, a solvent of similar size but with a molecular inversion centre. The structure of **5**·*p*-xylene (2:1) is isomorphous ($P\bar{1}$) and its crystal packing, unit-cell dimensions and volume are similar to those of the other clathrates (Fig. 3, Table 1). Interestingly, *p*-xylene is ordered and occupies a host channel that is of the same size as the cavity in the disordered structures (O···O distances in dimer synthon **4**: 2.62–2.65 Å, Table 2). This suggests that the latter reason, namely a mismatch of symmetry between the host and guest, is responsible for guest disorder with unsymmetrical

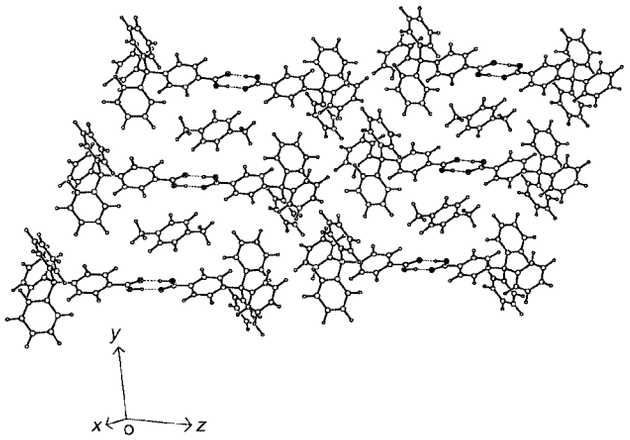

Fig. 3 Crystal structure of compound **5**·*p*-xylene down [100] with ordered guest molecules. The wheel-and-axle topology, zigzag tapes along [001] and the inclusion of solvent are similar in Figs. 1–3.

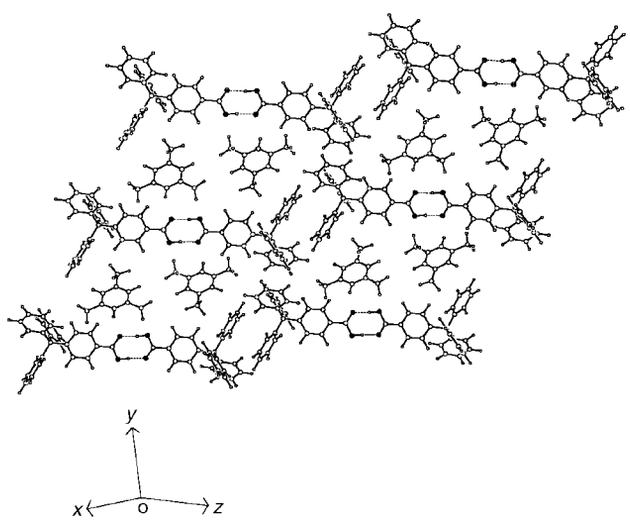

Fig. 4 Crystal structure of compound **5**·mesitylene down [100]. The voids contain two ordered guest molecules. Compare the zigzag tapes with Fig. 3. Notice that the phenyl–phenyl interactions along [001] are similar but the stacking of tapes along [010] is different.

solvents. Such a phenomenon is with precedent in the host–guest literature.[22]

Noting the recurrence of wheel-and-axle topology in the structures of acid **5**, recrystallisation was attempted from a bulkier aromatic solvent, mesitylene, to assess the cavity size. The supramolecular axis **4** (1.65 Å, 169.3°) is present in the crystal structure of **5**·mesitylene ($P\bar{1}$, $Z = 2$) but the host–guest stoichiometry is 1:1 instead of 2:1 (Fig. 4). The pore size in this structure has almost doubled (71 Å^2) compared to the xylene-type clathrates (*ca.* 42 Å^2).§ It is large enough to accommodate two ordered mesitylene molecules related by a crystallographic inversion centre. The ordered orientation of guests in **5**·mesitylene corroborates that if the guest symmetry matches the $P\bar{1}$ symmetry of the host lattice then the crystal structure will be fully ordered. The modulation of cavity area through different phenyl packing motifs is analysed below.

Unsolvated acid 5

Recrystallisation of acid **5** from nitromethane, a small non-aromatic solvent, provided crystals of the unsolvated, guest-free form in the orthorhombic space group, *Pbca*. A stereoview

§ Since the host channels are irregular in shape, the area was approximated as a sum of rectangles and triangles. Atoms were selected on the periphery of four acid molecules that form the channel and projected on a plane to calculate the cavity area.

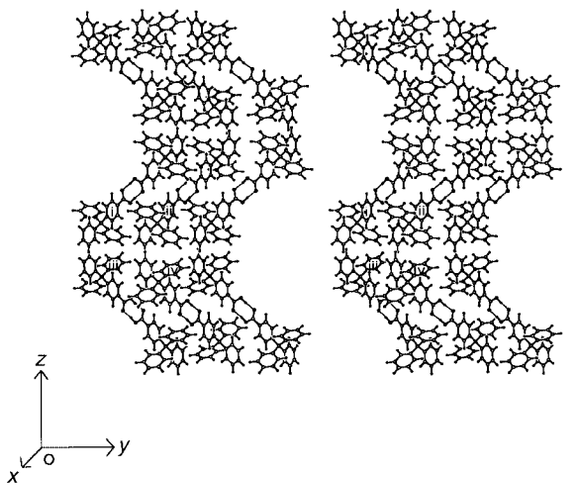

Fig. 5 Stereoview of acid **5** to show the self-inclusion of trityl groups in the voids created by the carboxylic acid dimer synthon. Molecules labeled i, iii and ii, iv are related by *a*-glide, molecules i, ii and iii, iv by the *b* glide, and i, iv and ii, iii by 2_1 along the *b*-axis.

of the structure (Fig. 5) shows the wave-like tapes along [001] between inversion- and *a*-glide-related molecules and the adjacent tapes along [010] between screw-axis and inversion-related molecules. In the structure of **5** a large number of adjacent phenyl rings, stabilised by the **off** and **ef** motifs,[21] are close-packed in the voids around the supramolecular axle **4** (1.68 Å, 169.6°). It may be noted that though the packing features of the solvated and single-component crystals of **5** are quite different, the structures bear close resemblance in terms of the hydrogen bonding and phenyl–phenyl synthons. The structure of unsolvated **5** may be compared with the 1:1 complex of 4-tritylphenol and triphenylphosphine oxide[23] in which the phenyl groups of triphenylphosphine fill the voids in the O–H···O inter-link region and the triphenyl groups of 4-tritylphenol are stabilised by the sextuple phenyl embrace.[21]

The analysis of inclusion compounds of **5** and its solvent-free form shows that $CO_2H\cdots CO_2H$ hydrogen bonding is a recurring recognition pattern, or supramolecular synthon, that mediates self-assembly and steers crystal packing in this family of structures. The weak C–H···O interactions (Table 2) between host–host and host–guest molecules additionally stabilise the crystal structures. The probabilities of formation (P_s) for 75 bimolecular hydrogen bonded motifs in organic crystal structures were analysed recently.[24] The P_s of dimer synthon **4** in monocarboxylic acids with no competing donors and acceptors is 95%.¶ The energy of the CO_2H dimer synthon is about 15 kcal mol^{-1}.[25] The repeated occurrence of the centrosymmetric dimer in the different crystal forms of acid **5** is therefore not totally unexpected because the synthon is robust and strong.

Phenyl packing and host cavity tuning

The packing orientations of phenyl rings in aromatic hydrocarbons as well as in other groups of compounds have been investigated by a number of researchers.[26] Specific attractive interactions between pairs of phenyl rings as identified in the crystal structures of triphenylphosphonium salts[21,26c] are of the offset face-to-face (**off**), edge-to-face (**ef**) and vertex-to-face (**vf**) type. These configurations have a significant structure-directing Coulombic attraction arising from the C(δ−)/H(δ+) polaris-

¶ This is the upper limit for P_s of motif 23 in ref. 24, the value being lower for all carboxylic acids without competing functional groups (91%) and, surprisingly, falls to 33% for all carboxylic acids with no restrictions imposed. In hindsight, formation of dimer synthon in the present acid is favoured by design because it is an aromatic, monocarboxylic acid.

Table 3 Phenyl–phenyl interactions in crystal structures of compound **5**

Guest	Intra-/ inter-tape	Offset face-to-face[a]/Å	Edge-to-face[a]/Å	Central C···C/Å	Cavity area/Å^2
p-Xylene	Intra	**off** 5.96	—[b]	8.84	42
	Inter	**off′** 4.92	ef 5.21	9.01	
Mesitylene	Intra	**off** 5.90	—[b]	8.03	71
	Inter	**off′** 4.20	—[b]	8.22	
None	Intra	**off** 5.97	ef 5.69	8.68	None
	Inter	—[b]	—[b]	14.26	

[a] Phenyl centroid-to-centroid distance. [b] No interaction could be found up to 8 Å distance.

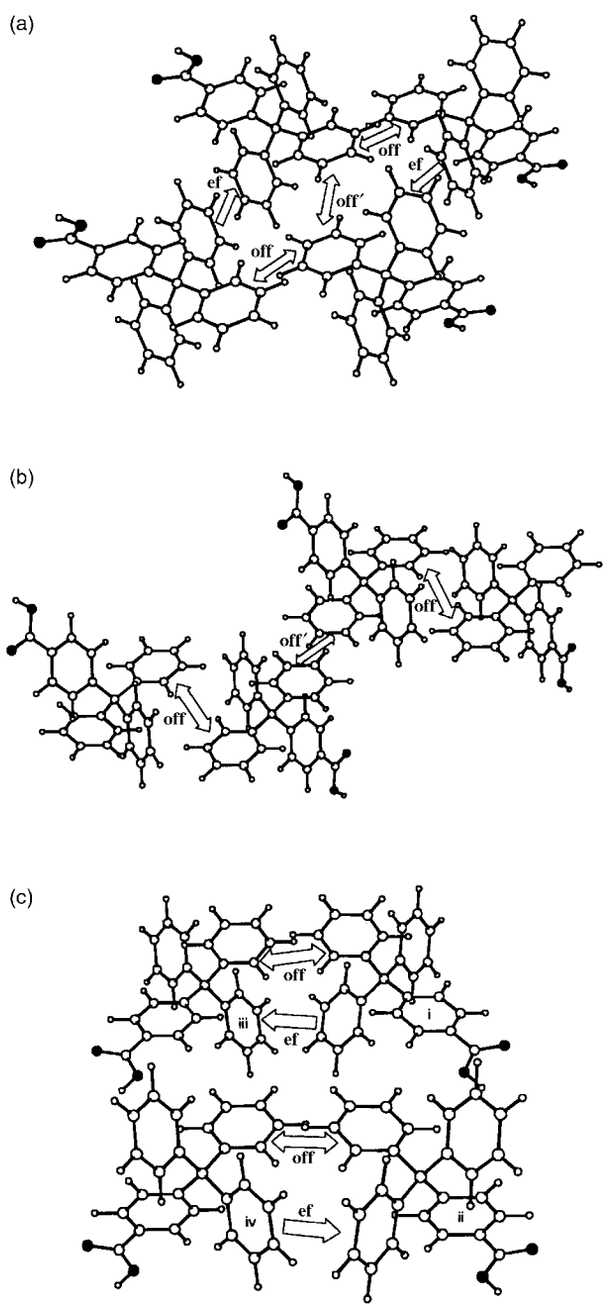

Fig. 6 Phenyl–phenyl interactions in the intra-tape (left to right) and inter-tape (up to down) regions: (a) **5**·*p*-xylene; (b) **5**·mesitylene; (c) unsolvated **5**. The different aromatic packing motifs lead to variation in cavity size with cross-sectional area of 42 Å^2 in (a), 71 Å^2 in (b) and none in (c). Labels i, ii, iii and iv in (c) are taken from Fig. 5.

ation in addition to the dispersion forces. The stabilisation from **off** and **ef** ring pairs is calculated to be 2–4 kcal mol^{-1} for an inter-centroid separation of 5–7 Å which increases to 5 kcal mol^{-1} for the **off** interaction at 4 Å separation.[21] Though by themselves weak, these long-range electrostatic interactions are able to steer crystal packing because clusters of phenyl rings contain several pairs of such interactions which together make a significant contribution to the stability of that particular motif. For example, double phenyl and sextuple phenyl embraces have calculated total energies of *ca.* 10 and 20 kcal mol^{-1}, respectively,[21,26c] which are comparable to those of conventional hydrogen bonds and, specifically, to the carboxy dimer synthon in these structures.

Phenyl packing motifs in the ordered crystal structures, **5**·*p*-xylene, **5**·mesitylene and pure **5**, are enlarged from Figs. 3–5 and shown for four acid molecules in Fig. 6a–c to analyse the geometries of phenyl–phenyl interactions within (intra) and between (inter) the zigzag tapes of acid molecules. In Fig. 6a and 6b inversion-related, intra-tape molecules are shown above and the translation-related, inter-tape pair is shown below. In Fig. 6c the glide-related molecules (i and iii) of wave-like tapes along [001] are shown above and the screw-axis related pair (iv and ii, respectively) along [010] is shown below.

The phenyl rings of acid molecules within a tape and between the tapes are oriented parallel and present in an offset face-to-face motif (**off**, intra-tape and **off′**, inter-tape) in **5**·mesitylene and **5**·*p*-xylene. The intra-tape **off** interactions in these two structures have inter-centroid separations of 5.90 and 5.96 Å while the inter-tape **off′** interaction is significantly shorter in **5**·mesitylene (4.20 *vs.* 4.92 Å, Table 3). The longer **off′** interaction in the xylene solvate is compensated by additional stabilisation from the inter-tape **ef** contact (5.21 Å) which is absent in the mesitylene clathrate. While the intra-tape **off** motifs have similar metrics in hosts with different pore sizes, the inter-tape motifs, **off′** and **ef**, have different geometries depending on the pore size. Further, the contact area between phenyl rings is inversely related with pore size: the mesitylene clathrate has a large channel area, minimum phenyl contact surface and stronger aromatic interactions while the xylene prototype has a smaller cavity through a profusion of weaker phenyl–phenyl interactions over a larger surface area. Thus, the adaptive behaviour of host **5**, that is its ability to form channels of different area (42 and 71 Å^2) depending on the solvent size, is rationalised by an understanding of the aromatic interactions. In effect, robustness, or the recurring zigzag tape pattern, is ascribed to the carboxy dimer synthon and adaptivity, or the tuning of pore volume, to the profusion of phenyl–phenyl motifs. Such a dual and non-intersecting property exhibited by acid **5** could be advantageous in the design of new host–guest materials.[27]

The word 'robust' as used here is meant to emphasise the repeated occurrence of the hydrogen bonded dimer **4** in the host structure despite variation in the guest species. This is different from a robust lattice, that is the ability of the host framework to retain its architecture and topology upon exchange or removal of guest.[28] The former meaning of robust relates to the structure-determining role of a supramolecular synthon within a family of crystal structures[29] while the latter meaning refers to the physical strength of the host lattice. This distinction between the two meanings of 'robust' must be made clear, especially in papers which deal with crystal engineering *and* host–guest issues.

Table 4 Crystal Packer (Cerius²) calculations on compound **5**

Guest	Cell (*a*, *b*, *c*/Å; *α*, *β*, *γ*/deg)	Crystal energy/kcal mol^{-1} VdW (%)[a]	Coulomb (%)[a]	H bond (%)[a]	Cell/Molecule[b]	*Z*[c]
p-Xylene	7.17, 8.94, 19.11	−90.33	−9.67	−7.42	−107.42	2 H + 1 G
	84.8, 87.7, 66.4	(86.2)	(8.6)	(5.2)	−46.7	
Mesitylene	7.28, 13.39, 14.15	−110.71	−11.08	−6.73	−128.52	2 H + 2 G
	78.1, 83.0, 85.1	(84.1)	(9.0)	(6.9)	−48.0	
None	7.31, 15.52, 33.78	−290.15	−68.80	−20.28	−379.23	8 H
	90.0, 90.0, 90.0	(76.5)	(18.1)	(5.4)	−47.4	

[a] Value in parentheses is percentage of total energy. [b] Energy per molecule of compound **5** calculated using the equation (Energy of cell ÷ Formula weight of cell) × Formula weight of **5**. [c] Contents of the unit cell. H = host, G = guest.

Examination of the unsolvated form of acid **5** is instructive. The dimer synthon **4** is present here but the phenyl packing motifs are somewhat different. Intra-tape packing (along [001]) is of the **off** and **ef** type (5.97 and 5.69 Å) but there are no short contacts in the inter-tape region along [010] (C···C > 14 Å, Table 3).‖ The intermolecular distances between the central sp^3 C···C atoms of trityl groups (8–9 Å) in the unsolvated and inclusion forms of **5** are much shorter than the diameter of a trityl group (13.0 Å) suggesting that the aromatic interactions in these structures are attractive and stabilising in nature.

The tendency to strive towards close packing is achieved with equal efficiency in the adduct crystals and in the guest-free form of compound **5** since their packing coefficients, C_k, are comparable (0.65–0.70, Table 1). The expulsion of solvent to form single-component crystals, the normal outcome of crystallisation for 85% of neutral organic molecules,[30] does not routinely occur for **5**. Instead, solvents are readily included during self-assembly, possibly because enclathration leads to energetically stable crystal structures. To verify this hypothesis, crystal energies were computed for **5**·*p*-xylene, **5**·mesitylene and unsolvated **5** with the Crystal Packer program (Cerius²)[31] by energy minimisation of the experimental crystal structures. The total energy per unit cell and the contributions from van der Waals, Coulomb and hydrogen bonding are listed in Table 4. The energies per molecule** in the three crystal structures are 46.7, 48.0 and 47.4 kcal mol^{-1} indicating that the various crystal forms of **5** examined in this study have energies within a narrow kcal mol^{-1} range. Since the constituents of each crystal are different (*Z* column), a more useful and meaningful parameter is the percentage contribution to crystal energy (given in parentheses in Table 4). O–H···O hydrogen bonding is of a similar magnitude in the three structures and so is its contribution to the total energy (5–7%). The Coulomb component in unsolvated **5** is twice as large when compared with its clathrates (18 *vs*. 9%) while the van der Waals contribution is higher in the solvated crystals (84–86 *vs*. 76%). The larger contribution from Coulomb interactions to the unsolvated crystal is because of the profusion of phenyl–phenyl packing motifs and C–H···O interactions (Table 2). The van der Waals component is higher in the host–guest structures because the filling of interstitial voids is based on molecular shape features rather than on specific, directional and electrostatic interactions. Thus, the observed hydrogen bonding and phenyl packing motifs in the crystal structures of **5** are substantiated by the Cerius² energy calculations.

‖ The van der Waals diameter of the Ph_3C group is calculated to be 13.0 Å by adding the van der Waals radius of an H atom to the central C to *p*-phenyl H atom distance (1.2 + 5.3 = 6.5 Å) in the crystal structure of Ph_4C (TEPHME03). This gives an upper bound of the van der Waals diameter of Ph_3C because these groups are not spherical.

** Since the number and nature of molecules per unit cell are different (*Z* column, Table 4), three in **5**·*p*-xylene, four in **5**·mesitylene and eight in unsolvated **5**, the total energies were normalised to per molecule of **5** based on formula weight.

Related host frameworks

The multi-component host **5** is compared with other examples of all-organic†† wheel-and-axle systems with a non-covalent axis. In the acetone clathrate of gossypol[32] the host binaphthyl groups adopt a V-shape conformation with one naphthyl ring π-stacked on the centrosymmetrically related neighbour to form a 'flattened axle', while the other naphthyl rings of the dimer constitute the wheels (Fig. 7a). A 'bloated axle' is formed in 9-phenylfluorene-9-carboxylic acid[33] by the two EtOH molecules that interrupt the centrosymmetric carboxylic acid dimer and also fill the voids (Fig. 7b). The six-component supermolecule formed by the co-crystallisation of ditopic crown ether and dibenzylammonium carboxylic acid[19] is an example of a 'double axle' mediated through the carboxy dimer supramolecular synthon (Fig. 7c). In triphenylacetic acid,[34] the sextuple phenyl embrace between the trityl groups dictates the threefold symmetry in the crystal with the result that the carboxy dimers are disordered over three orientations rotated by 120° around the supramolecular axis (Fig. 7d). While this structure displays the wheel-and-axle architecture, the voids are filled by phenyl rings and no guest species is included. In contrast to these cases, acid **5** provides a clear and unambiguous visualisation of the 'wheel-and-supramolecular-axle' concept and exemplifies its potential in host–guest chemistry.

DSC and TG analysis

Differential scanning calorimetry (DSC) and thermal gravimetry (TG) measurements were carried out on the crystalline samples, **5**·xylene, **5**·PhCl, **5**·*p*-xylene and **5**·mesitylene. In each case, the solvent is lost close to its boiling point in the TG analysis. The observed weight loss in **5**·xylene (2:1) between 130 and 160 °C is 11.16%; the calculated weight loss is 14.56%. The difference between calculated and observed weight loss could be due to the volatile nature of xylene and/or because the stoichiometry of the complex may not be exactly 2:1. The endotherm at >130 °C in the DSC trace corresponds to the escape of solvent from the host lattice which is followed by the melting of pure **5** at 270 °C. The DSC and TG traces for **5**·xylene are displayed in Fig. 8.

Conclusions

Wheel-and-axle terphenyl **2** served as the inspiration for its supramolecular surrogate, acid **5**, akin to arguments employed for hexakis(aryloxy)benzenes (molecules) and Piedfort Units (supermolecules).[35] These examples highlight the equivalence of molecular and supramolecular synthons in molecules and crystals and the advantage of exploiting their topological similarity in retrosynthesis.[29] In the present context, a host molecule that is difficult to synthesize could be systematically studied *via* its supramolecular equivalent through an advance in

†† For an organometallic wheel-and-axle system, see ref. 1(b), pp. 602–605.

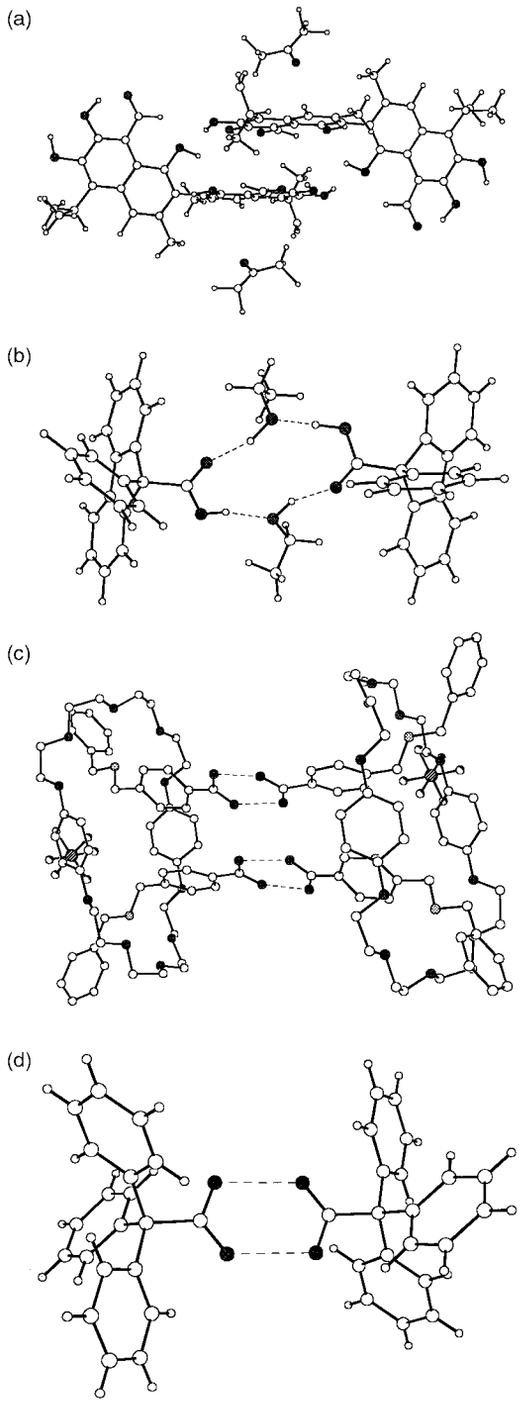

Fig. 7 Some approximate wheel-and-axle type crystal structures: (a) flattened axle; (b) bloated axle; (c) double axle; (d) guest-free axle.

conceptual design. It is therefore reassuring that the structure and function of multi-component host **5** is analogous to its molecular sibling **2**.‡‡

We have shown the utility of 4-tritylbenzoic acid **5** as a new two-component host to obtain wheel-and-axle adducts with different aromatic guests. The robust carboxy dimer supramolecular synthon produces an isomorphous series of clathrates for guests of similar size/shape, while the pore volume is engineered by the multiple phenyl–phenyl motifs. This study gives an idea of the extent to which the host–guest structures are isomorphous or adaptive to an isomeric architecture depending on the guest species, thereby demonstrating the generality of this new host scaffold. Ongoing studies will examine issues such as absorption of solvent by the apohost, selective enclathration with mixtures of solvents, guest exchange, and enthalpy of guest release from the host lattice.

‡‡ This was verified through Crystal Packer calculations (Cerius[2]). The carboxy dimer synthon in **5**·xylene was replaced by a phenyl connector and the structure minimised. There was no substantial change in the crystal packing and the arrangement of solvent molecules after energy minimisation of the putative structure, **2**·xylene (ref. 20a).

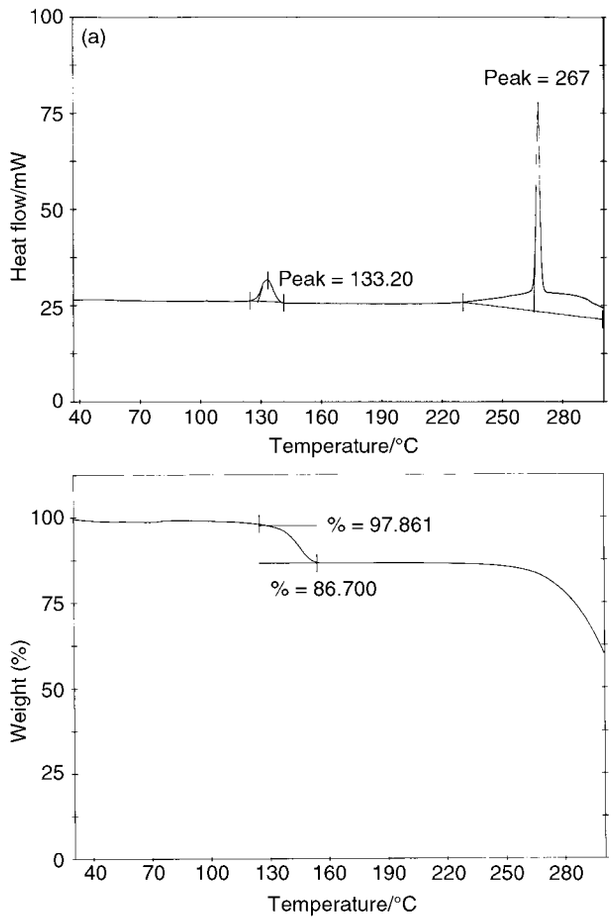

Fig. 8 DSC (a) and TG (b) plots of **5**·xylene (mixed). The endotherm at >130 °C in the DSC trace corresponds to solvent loss in the TG analysis.

Finally, a general comment is made about the classification of solute–solvent crystals as solvates, clathrates, host–guest or inclusion compounds. The definition of pseudopolymorphism was expanded recently to cover these related situations. Pseudopolymorphs are solvated forms of a compound which have different crystal structures and/or differ in the nature of the included solvent.[36] The scope and meaning of terms such as pseudopolymorph, solvate, clathrate and inclusion compound are intersecting and one term may be more appropriate than another, depending on the particular chemical situation.

Experimental

Synthesis

IR and NMR spectra were recorded on JASCO 5300 and Bruker ACF 200 instruments. All solvents and reagents were dried and distilled prior to use. Spectral characteristics of the synthesized compounds showed satisfactory match with literature data.[18]

4-(Triphenylmethyl)iodobenzene 6. A mixture of trityl alcohol (520 mg, 2.0 mmol), aniline (0.28 ml, 3.0 mmol), conc. HCl (0.9 ml, 11.0 mmol) and glacial AcOH (10 ml) were heated at reflux for 48 h. The intermediate anilinium salt was isolated by precipitation and filtration at room temperature. The residue was dissolved in 15 ml of EtOH and conc. H_2SO_4 (1 ml, 18.4 mmol)

was added. Diazotisation at −10 °C with isopentyl nitrite (0.6 ml, 4.4 mmol) and addition of KI (1.33 g, 8.0 mmol) afforded the iodo derivative **6** which was filtered off and purified by column chromatography (223 mg, 25%). mp 232 °C. IR (cm^{-1}): 3053, 1593, 1481, 1440, 1182, 1033, 1001, 891, 817, 750, 700, 630, 524. ^{1}H NMR (δ, $CDCl_3$): 7.57 (d, *J* 8, 2 H), 6.96 (d, *J* 8 Hz, 2 H), 7.27–7.17 (m, 15 H).

4-(Triphenylmethyl)cyanobenzene 7. A mixture of CuCN (270 mg, 3.0 mmol) and iodobenzene **6** (267 mg, 0.6 mmol) in dry DMF (2 ml) was heated at 140 °C for 3 h. A 1:1 mixture of EtOH and 60% aq. $FeCl_3$ solution was added (5 ml) at rt. The mixture was heated to boiling point briefly (2 min), cooled to rt and then added with stirring to 2.5 M HCl (30 ml). The product was extracted with CH_2Cl_2 (30 ml) and the organic extracts were washed with saturated aq. Na_2EDTA solution. The organic layer was dried with $MgSO_4$, filtered and concentrated to provide 136 mg (65%) of compound **7**. mp 220 °C. IR (cm^{-1}): 3055, 2226, 1593, 1489, 1442, 1280, 1184, 1033, 827, 748, 700, 632, 563. ^{1}H NMR (δ, $CDCl_3$): 7.55 (d, *J* 8, 2 H), 7.37 (d, *J* 8 Hz, 2 H), 7.27–7.15 (m, 15 H).

4-(Triphenylmethyl)benzoic acid 5. A mixture of cyanobenzene **7** (200 mg, 0.6 mmol), KOH (160 mg, 2.8 mmol) and ethylene glycol (4 ml) was refluxed for 6 h, then cooled to rt, diluted with water and extracted with CH_2Cl_2. The organic extracts were washed with dil. HCl, dried with $MgSO_4$ and concentrated to give the acid **5** (72 mg, 35%) which was recrystallised from CH_2Cl_2. mp 267 °C. IR (cm^{-1}): 3028, 1741, 1678, 1597, 1491, 1429, 1296, 1035, 854, 750, 700, 632, 526. ^{1}H NMR (δ, $CDCl_3$): 7.96 (d, *J* 8, 2 H), 7.35 (d, *J* 8 Hz, 2 H), 7.29–7.15 (m, 15 H).

X-Ray crystallography

Single crystals suitable for X-ray diffraction were obtained by recrystallisation of acid **5** from the appropriate guest, used as a solvent. All crystals were needle shaped and colourless. Data were collected with the ω-scan technique[37] on a Rigaku AFC7R diffractometer or on a Bruker SMART CCD area detector[38] using Mo-Kα radiation ($\lambda = 0.71073$ Å) at 294 K and absorption correction applied to the reflections based on ψ-scan data[39] (AFC7R) or using the SADABS program[40] (SMART). Structure solutions and refinements were routinely performed (SHELX packages).[41] The hydrogen atoms of aryl groups were generated with idealised geometries and isotropically refined using a riding model. H atoms of CO_2H groups were located from the difference density maps. Refinements of co-ordinates and anisotropic thermal parameters of all non-hydrogen atoms were carried out by the full-matrix least squares method. Final *R* indices and crystallographic parameters are listed in Table 1. All O–H and C–H distances are fixed at neutron-normalised distances, 0.983 and 1.083 Å respectively, for the hydrogen-bond geometries in Table 2. The treatment of guest disorder is summarised in Table 5. In all structures the alternative orientations of guest molecule are related by crystallographic inversion centres as illustrated in Fig. 9.

CCDC reference number 188/237.

See http://www.rsc.org/suppdata/p2/a9/a909827e/ for crystallographic files in .cif format.

Cerius^2 calculations

Crystal energy calculations were carried out in the Cerius^2 suite of programs (version 3.9). Using the experimental crystal structures as input, the electrostatic potential (ESP) charges were determined (AM1, MOPAC). The geometries were not optimised as this would lead to a loss of molecular symmetry. ESP charges were assigned to the molecules, the appropriate crystal system built in Crystal Packer and the lattice energies calculated

Table 5 Crystal data collection, structure solution, refinement and guest disorder

	5·Xylene	**5**·PhCl	**5**·*o*-Xylene	**5**·*m*-Xylene	**5**·*p*-Xylene	**5**·Mesitylene	**5**·Anisole	**5**·PhBr	**5**·$PhNO_2$	Unsolvated **5**
Data collection	Rigaku	Rigaku	Rigaku	Rigaku	Rigaku	Rigaku	Rigaku	Bruker	Rigaku	Rigaku
Solution	SHELXS 86	SHELXS 86	SHELXS 86	SHELXS 86	SHELXS 97	SHELXS 86	SHELXS 86	SHELXS 97	SHELXS 97	SHELXS 86
Refinement	SHELXL 93	SHELXL 93	SHELXL 93	SHELXL 93	SHELXL 97	SHELXL 93	SHELXL 93	SHELXL 97	SHELXL 97	SHELXL 93
Guest disorder model	*p*- and *m*-xylene in 1:2 ratio; this mimics *o*-xylene	Pseudo-inversion centre at (0.5, 0.5, 0.5); C27–C32 fixed as hexagon	Mimics a naphthalene	One of the Me C overlaps with ring C of related molecule	None	None	Mimics a naphthalene; oxygen could not be located	Similar to PhCl; pseudo-inversion centre at (1, 0, 0)	Mimics 1,5-disubstituted naphthalene; NO_2 groups overlap, N and O could not be located	None
S.o.f.[a]	C27–C33 0.50 each, C34 0.33, C35 0.17	C27–C32 0.5 each, Cl 0.25 (with this site occupancy of chlorine, a.d.p.[b] of Cl is reasonable	C29, C30, H29, H30 0.5 each; C27, C28, C31, H28, H31 1.0 each	C27, C28, C30 1.0 each; C29, C31 0.5 each			C27–C31, H28–H31 1.0 each	C27–C31, Br 0.5 each	C27–C31, O3 0.5 each	

[a] Site-occupancy factor. [b] Atomic displacement parameter.

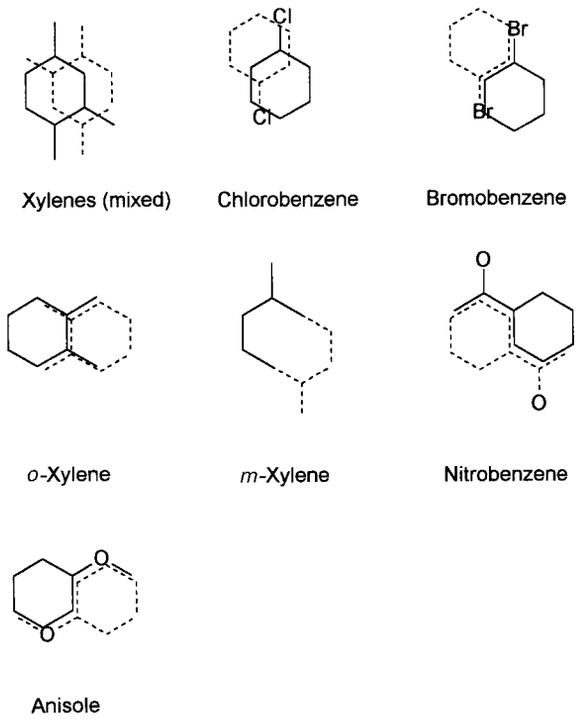

Fig. 9 Modelling of guest disorder in clathrates of host **5**. Molecules with solid and dashed lines represent the two orientations of a guest species about an inversion centre.

of the minimised structures (Table 4). All calculations were performed using standard program default parameters.

Acknowledgements

This project is funded by the Department of Science and Technology (SP/S1/G29/98), Government of India and the Hong Kong Research Grants Council Earmarked Grants (CUHK 4206/99P). We thank Dr V. Smith and Prof. L. R. Nassimbeni (University of Cape Town, South Africa) for DSC and TG measurements and Prof. G. R. Desiraju (University of Hyderabad) for helpful discussions.

References

1 (*a*) E. Weber, in *Kirk-Othmer Encyclopedia of Chemical Technology*, 4th edn., ed. J. I. Kroschwitz, John Wiley, New York, 1995, vol. 14, pp. 122–154; (*b*) *Comprehensive Supramolecular Chemistry*, eds. D. D. MacNicol, F. Toda and R. Bishop, Pergamon, Oxford, 1996, vol. 6; (*c*) R. Bishop, *Chem. Soc. Rev.*, 1996, **25**, 311; (*d*) Y. Aoyama, *Top. Curr. Chem.*, 1998, **198**, 131; (*e*) O. M Yaghi, H. Li, C. Davis, D. Richardson and T. L. Groy, *Acc. Chem. Res.*, 1998, **31**, 474; (*f*) L. R. MacGillivray and J. L. Atwood, *Angew. Chem.*, *Int. Ed.*, 1999, **38**, 1018.

2 (*a*) M. Simard, D. Su and J. D. Wuest, *J. Am. Chem. Soc.*, 1991, **113**, 4696; (*b*) K. Endo, T. Sawaki, M. Koyanagi, K. Kobayashi, H. Masuda and Y. Aoyama, *J. Am. Chem. Soc.*, 1995, **117**, 8341; (*c*) M. Sugahara, K. Sada and M. Miyata, *Chem. Commun.*, 1999, 293; (*d*) D. Hashizume and Y. Ohashi, *J. Chem. Soc.*, *Perkin Trans. 2*, 1999, 1689.

3 (*a*) A. T. Ung, D. Gizachew, R. Bishop, M. L. Scudder, I. G. Dance and D. C. Craig, *J. Am. Chem. Soc.*, 1995, **117**, 8745; (*b*) K. Endo, T. Ezuhara, M. Koyanagi, H. Masuda and Y. Aoyama, *J. Am. Chem. Soc.*, 1997, **119**, 499; (*c*) M. R. Caira, A. Horne, L. R. Nassimbeni and F. Toda, *J. Chem. Soc.*, *Perkin Trans. 2*, 1997, 1717; (*d*) K. Biradha, D. Dennis, V. A. MacKinnon, C. V. Krishnamohan Sharma and M. J. Zaworotko, *J. Am. Chem. Soc.*, 1998, **120**, 11894; (*e*) R. Thaimattam, D. S. Reddy, F. Xue, T. C. W. Mak, A. Nangia and G. R. Desiraju, *J. Chem. Soc.*, *Perkin Trans. 2*, 1998, 1783.

4 S. R. Batten and R. Robson, *Angew. Chem.*, *Int. Ed.*, 1998, **37**, 1460.

5 G. R. Desiraju, *Angew. Chem.*, *Int. Ed. Engl.*, 1995, **34**, 2311.

6 G. A. Jeffrey and W. Saenger, *Hydrogen Bonding in Biological Structures*, Springer-Verlag, Berlin, 1991; G. A. Jeffrey, *An Introduction to Hydrogen Bonding*, Oxford University Press, Oxford, 1997.

7 G. R. Desiraju and T. Steiner, *The Weak Hydrogen Bond in Structural Chemistry and Biology*, Oxford University Press, Oxford, 1999.

8 A. T. Ung, R. Bishop, D. C. Craig, I. G. Dance and M. L. Scudder, *Tetrahedron Lett.*, 1993, **49**, 639.

9 E. Weber, T. Hens, O. Gallardo and I. Csöregh, *J. Chem. Soc.*, *Perkin Trans. 2*, 1996, 737.

10 B. Ibragimov, K. Beketov, K. Makhkamov and E. Weber, *J. Chem. Soc.*, *Perkin Trans. 2*, 1997, 1349; K. Beketov, E. Weber, J. Seidel, K. Köhnke, K. Makhkamov and B. Ibragimov, *Chem. Commun.*, 1999, 91.

11 F. Toda and T. Tanaka, *Tetrahedron Lett.*, 1988, **29**, 551; E. Weber and C. Wimmer, *Chirality*, 1993, **2**, 123.

12 L. R. MacGillivray and J. L. Atwood, *J. Am. Chem. Soc.*, 1997, **119**, 6931; G. W. Orr, L. J. Barbour and J. L. Atwood, *Science*, 1999, **285**, 1049; G. Ferguson, C. Glidewell, A. J. Lough, G. D. McManus and P. R. Meehan, *J. Mater. Chem.*, 1998, **2**, 2339.

13 C. B. Aakeröy, A. M. Beatty and D. S. Leinen, *Angew. Chem.*, *Int. Ed.*, 1999, **38**, 1815.

14 J. A. Swift, A. M. Pivovar, A. M. Reynolds and M. D. Ward, *J. Am. Chem. Soc.*, 1998, **120**, 5887; C. C. Evans, L. Sukarto and M. D. Ward, *J. Am. Chem. Soc.*, 1999, **121**, 320; K. Sada, K. Yoshikawa and M. Miyata, *Chem. Commun.*, 1998, 1763.

15 See ref. 1(*b*): pp. 14 and 15; 310–313; 467–470; 602–605.

16 (*a*) N. Hayashi, Y. Mazaki and K. Kobayashi, *J. Chem. Soc.*, *Chem. Commun.*, 1994, 2351; (*b*) H. Hart, L.-T. Lin and D. L. Ward, *J. Am. Chem. Soc.*, 1984, **106**, 4043; (*c*) F. Toda and K. Akagi, *Tetrahedron Lett.*, 1968, 3695; (*d*) M. R. Caira, L. R. Nassimbeni, F. Toda and D. Vujovic, *J. Chem. Soc.*, *Perkin Trans. 2*, 1999, 2681.

17 T. Minami, K. Nishimura, I. Hirao, H. Suganuma and T. Agawa, *J. Org. Chem.*, 1982, **47**, 2360.

18 M. Grimm, B. Kriste and H. Kurreck, *Angew. Chem.*, *Int. Ed. Engl.*, 1986, 25, 1097; B. F. Hoskins and R. Robson, *J. Am. Chem. Soc.*, 1990, **112**, 1546.

19 P. R. Ashton, A. N. Collins, M. C. T. Fyfe, S. Menzer, J. F. Stoddart and D. J. Williams, *Angew. Chem.*, *Int. Ed. Engl.*, 1997, **36**, 735.

20 (*a*) R. K. R. Jetti, S. S. Kuduva, D. S. Reddy, F. Xue, T. C. W. Mak, A. Nangia and G. R. Desiraju, *Tetrahedron Lett.*, 1998, **39**, 913; (*b*) A. Anthony, G. R. Desiraju, R. K. R. Jetti, S. S. Kuduva, N. N. L. Madhavi, A. Nangia, R. Thaimattam and V. R. Thalladi, *Cryst. Eng.*, 1998, **1**, 1.

21 I. Dance and M. Scudder, *Chem. Eur. J.*, 1996, **2**, 481.

22 T. Imakubo, T. Matuyama, H. Sawa and K. Kobayashi, *Chem. Commun.*, 1998, 2021; A. J. Matzger, M. Shim and K. P. C. Vollhardt, *Chem. Commun.*, 1999, 1871; K. K. Makhkamov, B. T. Ibragimov, E. Weber and K. M. Beketov, *J. Phys. Org. Chem.*, 1999, **12**, 157.

23 R. K. R. Jetti, H.-C. Weiss, V. R. Thalladi, R. Boese, A. Nangia and G. R. Desiraju, *Acta Crystallogr.*, *Sect. C*, 1999, **55**, 1530.

24 F. H. Allen, W. D. S. Motherwell, P. R. Raithby, G. P. Shields and R. Taylor, *New J. Chem.*, 1999, 25.

25 A. Gavezzotti and G. Fillipini, *J. Phys. Chem.*, 1994, **98**, 4831; A. T. Hagler, P. Dauber and S. Lifson, *J. Am. Chem. Soc.*, 1979, **101**, 5131.

26 (*a*) G. R. Desiraju and A. Gavezzotti, *J. Chem. Soc.*, *Chem. Commun.*, 1989, 621; (*b*) C. A. Hunter, *Chem. Soc. Rev.*, 1994, **23**, 101; (*c*) I. Dance and M. Scudder, *New J. Chem.*, 1998, 481.

27 G. R. Desiraju, *Curr. Opinion Solid State Mater. Sci.*, 1997, **2**, 451; H.-B. Bürgi, J. Hulliger and P. J. Langley, *Curr. Opinion Solid State Mater. Sci.*, 1998, **3**, 425; P. J. Langley and J. Hulliger, *Chem. Soc. Rev.*, 1999, **28**, 279.

28 P. Brunet, M. Simard and J. D. Wuest, *J. Am. Chem. Soc.*, 1997, **119**, 2737.

29 R. K. R. Jetti, F. Xue, T. C. W. Mak and A. Nangia, *Cryst. Eng.*, 1999, **2**, 215.

30 A. Nangia and G. R. Desiraju, *Chem. Commun.*, 1999, 605.

31 Cerius^2, Molecular Simulations Inc., San Diego (USA) and Cambridge (UK).

32 S. A. Talipov, B. T. Ibragimov, G. N. Tischenko and T. F. Aripov, *Kristallografiya*, 1989, **34**, 327 (*Chem. Abstr.*, 1989, **110**, 223061m).

33 E. Weber, N. Dörphinghaus and Csöregh, *J. Chem. Soc.*, *Perkin Trans. 2*, 1990, 2167.

34 B. Kahr and R. L. Carter, *Mol. Cryst. Liq. Cryst. Sci. Technol.*, *Sect. A*, 1992, **219**, 79.

35 A. D. U. Hardy, D. D. MacNicol and D. R. Wilson, *J. Chem. Soc.*, *Perkin Trans. 2*, 1979, 1011; A. S. Jessiman, D. D. MacNicol, P. R. Mallinson and I. Vallance, *J. Chem. Soc.*, *Chem. Commun.*, 1990, 1619; D. D. MacNicol and G. A. Downing, in ref. 1(b), pp. 421–464.

36 V. S. S. Kumar, S. S. Kuduva and G. R. Desiraju, *J. Chem. Soc.*, *Perkin Trans. 2*, 1999, 1069.

37 R. A. Sparks, in *Crystallographic Computing Techniques*, ed. F. R. Ahmed, Munksgaard, Copenhagen, 1976, p. 452.

38 Bruker SMART 5.0 and SAINT 4.0 for Windows NT: Area Detector Control and Integration Software, Bruker Analytical X-ray Instruments Inc., Madison, WI, 1998.
39 G. Kopfmann and R. Huber, *Acta Crystallogr.*, *Sect. A*, 1968, **24**, 348.
40 G. M. Sheldrick, SADABS: Program for Empirical Absorption Correction of Area Detector Data, University of Göttingen, 1996.
41 G. M. Sheldrick, SHELXS 86, *Acta Crystallogr.*, *Sect. A*, **46**, 467, 1990; SHELXL 93: A Program for the Refinement of Single Crystal Diffraction Data, University of Göttingen, 1993; SHELXS 97: Program for the Solution of Crystal Structures, University of Göttingen, 1997; SHELXL 97: Program for the Refinement of Crystal Structures, University of Göttingen, 1997.